

## Comparison of changes in micropores and mesopores in the wood cell walls of sapwood and heartwood

Jiangping Yin<sup>1,2</sup> · Kunlin Song<sup>1,3</sup> · Yun Lu<sup>1</sup> ·  
Guangjie Zhao<sup>2</sup> · Yafang Yin<sup>1</sup> 

Received: 4 February 2015 / Published online: 11 June 2015  
© Springer-Verlag Berlin Heidelberg 2015

**Abstract** The objective of this paper was to investigate size distribution of micropores and mesopores within the wood cell walls between sapwood and heartwood by using nitrogen adsorption method and to find out implications for the biological durability and further processing such as in drying and preservation treatment. The pore shape, specific surface area and pore size distribution of Chinese fir (*Cunninghamia lanceolata*) were evaluated using the hysteresis loops, Brunauer–Emmett–Teller (BET) and density functional theories, respectively. Both the sapwood and heartwood exhibited slit-shaped pores with regard to the H3 type of hysteresis loop of the isotherm. However, more mesopores were found in the sapwood, while the micropores increased with a decrease in mesopores in the heartwood. Furthermore, the earlywood and latewood in the sapwood had a higher BET-specific surface area (2.088 and 1.255 m<sup>2</sup> g<sup>-1</sup>, respectively) compared with the earlywood (1.058 m<sup>2</sup> g<sup>-1</sup>) and latewood (0.787 m<sup>2</sup> g<sup>-1</sup>) in the heartwood. This could be caused by an increase in depositions in the extractive that partly filled the mesopores of the heartwood cell walls during the transformation from the sapwood. Additionally, a larger amount of mesopores existed in the earlywood in comparison with the latewood in the sapwood. However, there was no significant difference in the amounts of the micropores and mesopores, when comparing the earlywood with the latewood in the heartwood.

---

✉ Yafang Yin  
yafang@caf.ac.cn; yinyafangcaf@gmail.com

<sup>1</sup> Wood Anatomy and Utilization Department, Research Institute of Wood Industry, Chinese Academy of Forestry, No.1Dongxiaofu, Beijing 100091, China

<sup>2</sup> College of Materials Science and Technology, Beijing Forestry University, No.35 East Qinghua Road, Beijing 100083, China

<sup>3</sup> School of Renewable Natural Resources, Louisiana State University, Baton Rouge, LA 70803, USA

## Introduction

Surrounded by sapwood, heartwood is formed in the inner part of trees. Compared with sapwood, heartwood has worse drying and permeability properties, but its density, strength and natural durability improve a great deal (Adam et al. 2002; Aguilera and Zamora 2009). To explain the mechanism of heartwood formation and the effect on the wood properties between the sapwood and heartwood, numerous aspects have previously been studied, including genetic expression, enzyme activity, cell death, the distribution of water and gases, as well as the shape, size and colour of heartwood (Dehon et al. 2002; Huang et al. 2010; Song et al. 2011; Nishida et al. 2014). Previous studies emphasized the solid fraction, i.e. the primary and secondary walls are principally composed of cellulose, hemicelluloses and lignin, where the stiff cellulose fibrils are embedded in a soft matrix that consists of hemicelluloses and lignin. However, little information about the pores that existed in the solid fraction was included in the studies on heartwood formation. Wood as a biopolymer with its cellular structure is anisotropic and extremely inhomogeneous. All wood technological processes such as drying, steaming or impregnation strongly depend not only on the physical properties of wood as a whole but also on the arrangement, structure and accessibility of the cell elements, such as vessels, tracheids, fibre tracheids, longitudinal parenchyma and rays. The quantitative determination of the wood pore structure is essential for its characterization (Zauer et al. 2014a).

Wood is a porous material (Stone 1964; Nakato 1973; Sawabe et al. 1973; Zauer et al. 2013). The pores in the wood can be divided into three categories according to the IUPAC classification, viz. macropores (pore size  $> 50$  nm), mesopores ( $2 \text{ nm} < \text{pore size} < 50$  nm) and micropores (pore size  $< 2$  nm). When it comes to the flow of fluids, the initial step is a flow of fluid from the exterior to the interior of the wood via vessels, tracheids and rays. The diameter of these large pores is within the range of 15–400  $\mu\text{m}$  (macropores), but they are interconnected by pits, whose pores have a diameter ranging from 0.4 to 30  $\mu\text{m}$  (macropores). Reaching the lumen of a fibre, the liquid begins to diffuse into the cell wall through pores with diameters of a few nanometres (micropores and mesopores) (Table 1). The wood cell wall exhibits porosity of molecular-scale dimensions due to the partial filling of space between the cellulose microfibrils by lignin, hemicelluloses and extractives. These pores are generally referred to as micropores and mesopores. It has previously been shown that the micropores and mesopores in the wood cell wall play an essential role in wood behaviour, including mechanical properties, dimensional stabilization, fibre shrinkage, wood drying, wood preservation, wood modification, chemical pulping and bleaching (Papadopoulos and Hill 2003; ÖstlundÅ et al. 2010; Borrega and Kärenlampi 2011; Zauer et al. 2014b). Thus, it has been shown that the micropores and mesopores have a strong influence on the physical, chemical and mechanical properties of wood material.

Among the various techniques for characterizing micropores and mesopores, the nitrogen adsorption method was considered to be a promising method, allowing the pore size and surface area of materials with cavities smaller than 50 nm to be

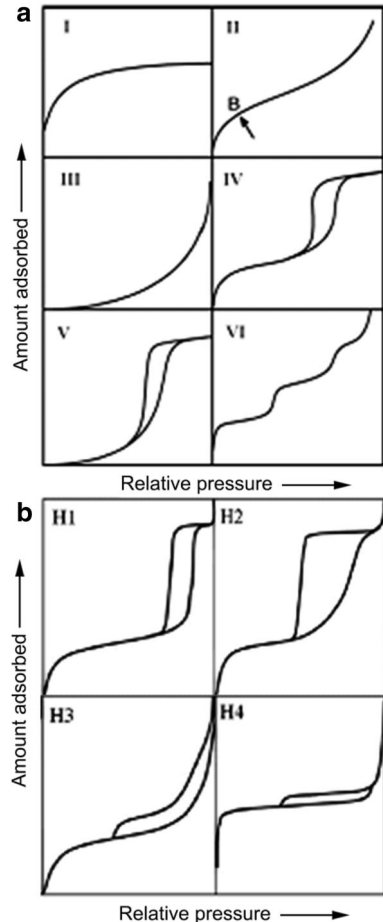
**Table 1** Pore parameters in wood

Pore types	Diameter	Pore shape	Tree species
<i>Macro</i>			
Resin canal <sup>a</sup>	50–300 $\mu\text{m}$	Cylindrical	Softwood
Vessel lumen <sup>b</sup>	40–250 $\mu\text{m}$	Cylindrical	Hardwood (diffuse porous wood)
Vessel lumen <sup>b</sup>	20–400 $\mu\text{m}$	Cylindrical	Hardwood (ring porous wood)
Tracheid lumen <sup>b</sup>	20–30 $\mu\text{m}$	Irregular cylindrical	Softwood
Wood fibre lumen <sup>b</sup>	$\sim 15 \mu\text{m}$	Cylindrical	Hardwood
Bordered pit chamber <sup>b</sup>	4–30 $\mu\text{m}$	Funnel-shaped	Softwood
Bordered pit aperture <sup>b</sup>	0.4–6 $\mu\text{m}$	Spherical	Softwood
<i>Macro/meso/micro</i>			
Pores in pit membrane <sup>a</sup>	10 nm–8 $\mu\text{m}$	Fine, Areole-shaped, Tubular-shaped	Softwood
Pores in cell wall <sup>a</sup>	1–100 nm	Slit-shaped	<i>Chamaecyparispisifera</i> , <i>Pterocaryarhoifolia</i> , <i>Paulownia tomentosa</i>
Pores in tension wood cell wall <sup>c</sup>	4–30 nm	Slit-shaped Ink bottle-shaped Funnel-shaped	<i>Populus</i> sp., <i>Sextoniarubra</i> <i>Ocoteaguyanensis</i> <i>Virolamichelii</i>
Microfibril clearance <sup>a</sup>	2–4.5 nm	Slit-shaped	<i>Piceaabies</i>
<i>Micro</i>			
Lignin <sup>d</sup>	0.3–0.6 nm	Slit-shaped	<i>Chamaecyparisohtuse</i> , <i>Faguscrenata</i>

References from <sup>a</sup> Sawabe et al. (1973), <sup>b</sup> Stone (1964), Stone and Scallan (1965), <sup>c</sup> Chang et al. (2009, 2011), <sup>d</sup> Nakatani et al. (2008), Kojiro et al. (2010)

calculated without changing the original features of the materials. Six types of isotherms and four types of hysteresis loops were identified, according to the IUPAC classification (Fig. 1). Stone and Scallan (1965) investigated the pore structure of wood by nitrogen adsorption and reported the effect of component removal on the pore structure of wood cell wall. Sawabe and Kitagawa (1978) studied widely the pore structures, size distribution, surface area and pore volume of swollen wood, dry wood, cellulose and lignin by nitrogen adsorption. According to Nakatani et al. (2008), the number of micropores decreased with the decrease in residual lignin, and micropores were hardly found in cellulose and hemicelluloses. To clarify the pore structure in cell walls of dry wood, the effects of heating history on pore volumes for both micropores and mesopores and the difference in pore volume between softwood Hinoki and hardwood Buna were investigated by Kojiro et al. (2010) using nitrogen adsorption and carbon dioxide adsorption. Chang et al. (2009) tried to characterize the mesopores in the tension wood. Measurements show that mesopores were high in tension wood with a typical thick G-layer, while they were much less with a thinner G-layer, sometimes no more than normal wood. Furthermore, the pore structures of wood cell wall derivatives, such as

**Fig. 1** IUPAC classifications of **a** adsorption isotherms and **b** hysteresis loops [reprinted from Sing et al. 1985, with kind permission from IUPAC]



lignocellulose aerogels and activated carbon fibres, were also analysed with the nitrogen adsorption method (Lu et al. 2012; Jin et al. 2014).

Despite the intensity of research activity done in this area, on the wood cell wall level, the differences and the mechanisms of the changes in micropores and mesopores when comparing the sapwood and heartwood have not been fully characterized and understood. A better understanding of the micropores and mesopores in the sapwood and heartwood is important, when it comes to tree cultivation, wood processing industry, and biofuel and biomaterial industry.

The aim of this study was to identify pore size distribution within the cell wall between the sapwood and heartwood by using nitrogen adsorption method (Autosorb iQ, Quantachrome USA), and the adsorption–desorption isotherm was obtained at the temperature of liquid nitrogen (77 K) on outgassed samples. The differences in the total pore volume ( $V_{\text{total}}$ ), BET-specific surface area ( $S_{\text{BET}}$ ), micropore surface area ( $S_{\text{micro}}$ ) and external surface area ( $S_{\text{ext}}$ ) between the sapwood and heartwood were investigated. The results will promote the understanding of the

effect and mechanism concerning the biological durability and further processing and also provide a scientific basis for the development of environmentally friendly wood products.

## Materials and methods

### Materials

Wood was selected from a 45-year-old plantation of Chinese fir [*Cunninghamia lanceolata* (Lamb.) Hook.], known for its high ratio of heartwood, good durability and important commercial value. Two blocks [30 mm (*L*) × 4 mm (*R*) × 10 mm (*T*)] were taken from growth rings 29 and 23 at breast height from the sapwood and heartwood separately (Fig. 2). The blocks used in this study all came from mature wood, based on the defined boundary between juvenile and mature wood for *C. lanceolata* (Yin et al. 2011a). Each block was divided into three pieces. One piece was divided into long sticks [5 mm (*L*) × 1 mm (*R*) × 1 mm (*T*)] and embedded in Spurr resin. Transverse sections (2 μm thick) of embedded wood samples were used for observation under a light microscope. One piece was sliced into radial sections (200 μm thick) for observation with a field emission scanning electron microscope (FE-SEM). Three small samples were taken from the last piece, and each small sample was divided into earlywood and latewood. All samples were then used for nitrogen adsorption measurement. Each of them weighed approx. 1 g. Furthermore, wood samples that were used in the FE-SEM and nitrogen adsorption measurement were supercritically dried to avoid collapse of pores in the wood cell walls.

### Supercritical drying

Firstly, wood samples were dehydrated by means of a series of graded ethanol (80, 90, 95, 100 %). The dehydrated samples were introduced into a Polaron 3100 apparatus, which was filled with liquid carbon dioxide (CO<sub>2</sub>). During supercritical drying, the liquid carbon dioxide was transformed into a supercritical fluid with a

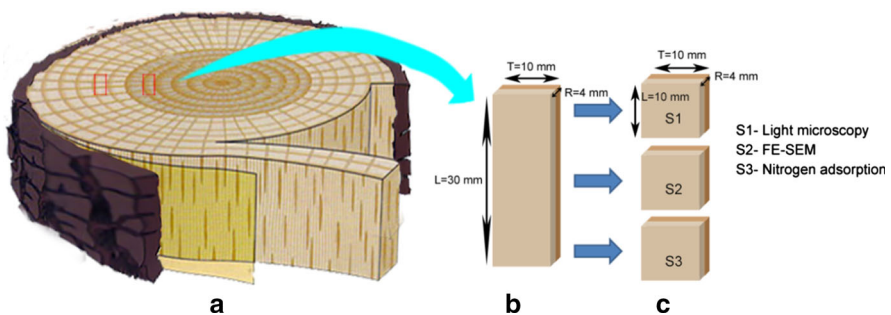


**Fig. 2** Diagram indicating the preparation of samples from a wood block of *Cunninghamia lanceolata* in order to make measurements utilizing light microscopy, FE-SEM and nitrogen adsorption

null surface tension by increasing the temperature beyond its critical point (304.25 K, 7.39 MPa), at which time the pressure was gradually released to allow gas to escape so that the wood samples were completely dried. In this way, any shrinkage due to capillary pressure was prevented, and the expectation was that the solid obtained, an aerogel, would reproduce the texture of the original hydrogel in a dry state.

### Light microscopy

Wood samples were dehydrated by means of a series of graded ethanol and embedded in Spurr resin. Transverse sections were cut with a glass knife, fixed on an ultramicrotome (LKB2188) and stained with a 1 % aqueous solution of toluidine blue for observation under a light microscope (OLYMPUS BX61, Japan).

### Field emission scanning electron microscope (FE-SEM)

Radial sections of wood samples were cut with a sliding microtome. The sections obtained were supercritically dried. Following drying, each specimen was coated with a thin layer of platinum using a sputter coater (JSM-5500LV) prior to examination in an FE-SEM (JSM-6301F, Japan).

### Nitrogen adsorption measurement

One gram of each sample was put into a sample cell and outgassed at 80 °C for at least 10 h under a high vacuum below  $10^{-5}$  Pa to remove any moisture or adsorbed contaminants from the sample surface. By means of the nitrogen adsorption isotherms, the pore volume was derived from the amount of adsorbed nitrogen at a relative pressure close to unity, assuming the pores were filled with liquid adsorbate. The shapes of pores were calculated using the hysteresis loops.  $V_{\text{total}}$  was calculated from the volume of the liquid nitrogen held at the relative pressure,  $P/P^0 = 0.99$ .  $S_{\text{BET}}$  of the samples was calculated using the Brunauer–Emmett–Teller (BET) equation.  $S_{\text{micro}}$  and  $S_{\text{ext}}$  were calculated with the t-plot method. The pore size distribution was calculated using the density functional theory (DFT).

One-way statistical analysis (ANOVA) was done on the datum to evaluate the differences between the sapwood and heartwood on the  $V_{\text{total}}$ ,  $S_{\text{BET}}$ ,  $S_{\text{micro}}$  and  $S_{\text{ext}}$  of the cell wall, by using SAS programme 9.0 (SAS Institute, Inc.). Each datum was calculated from three duplicated samples.

It should be noted that the pores in the wood were divided into three categories according to the IUPAC classification in this work to facilitate better communication between wood science and other research areas (Sing et al. 1985), although the macropores (10 to 400  $\mu\text{m}$  or greater), micropores (10 nm to 5  $\mu\text{m}$ ) and nanopores (below 10 nm) were classified in a different way according to some previous literature in wood science (Thygesen et al. 2010; Grigsby et al. 2013; Zauer et al. 2014b).

## Results and discussion

### Anatomical observations

The anatomical sections of the sapwood and heartwood are shown in Fig. 3. The cell walls in *C. lanceolata* were mainly composed of tracheid and ray parenchyma cells (Fig. 3a–b). Tracheid end walls in the sapwood and heartwood had a large area of connecting bordered pits, with a typical torus-margo anatomy in the pit membrane (Fig. 3c–d). The large-scale pores that were responsible for the reduced flow resistance were found in the pit membrane margo of sapwood (Fig. 3c). In contrast, the more amorphous material deposited on the pit membrane margo of heartwood, and the pore diameter was noticeably reduced (Fig. 3d). The narrow and smaller-scale pores created a high resistance to the flow in the heartwood pit membrane. This was confirmed by Gray et al. (1983).

The pit membrane in the sapwood consisted of celluloses, matrix and pectin. However, additional lignin-like and procyanidin polymers were found in the heartwood pit membrane (Bauch and Berndt 1973). The pores in the pit membrane

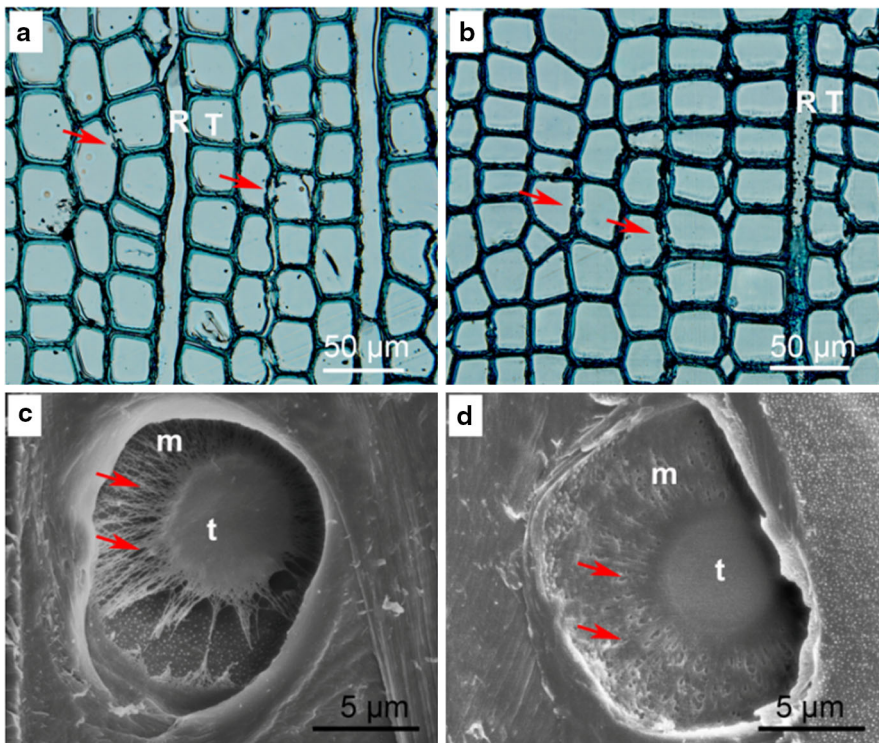


**Fig. 3** Light microscopy images of transverse sections of *Cunninghamia lanceolata*, showing bordered pits in **a** sapwood and **b** heartwood (arrows), Scale bar = 50  $\mu\text{m}$ . FE-SEM images of the border pit membrane of tracheids, demonstrating pores in **c** sapwood and **d** heartwood (arrows), Scale bar = 5  $\mu\text{m}$ . *T* tracheids, *R* ray parenchyma cells, *m* margo, *t* torus



might have been seriously blocked by the extractives occurring during transformation from the sapwood to heartwood (Qin et al. 2004). Therefore, it could be hypothesized that this might affect the morphological structure and distribution of micropores and mesopores in the wood cell walls, if the formation of the heartwood had influenced the pores in the pit membrane as a result of extractives.

### Adsorption–desorption isotherm and pore shape

The nitrogen adsorption–desorption isotherms of earlywood in sapwood (E-SW), latewood in sapwood (L-SW), earlywood in heartwood (E-HW) and latewood in heartwood (L-HW) are shown in Fig. 4. According to IUPAC classification (Fig. 1a), the isotherm of E-SW was intermediate between type II and type IV. Specifically, there was some adsorption under low relative pressure, where micropores were mainly filled in this stage, showing that micropores existed in the sample. The adsorption increased with an increase in relative pressure, where capillary condensation occurred at this stage. With high relative pressure, the adsorption increased rapidly and failed to reach adsorption saturation. The desorption isotherm did not coincide with the adsorption isotherm, and a hysteresis loop was observed. This obviously suggested the existence of mesopores and a certain amount of macropores in the E-SW (Zhang et al. 1997; Chang et al. 2011). A similar phenomenon was observed for the L-SW, E-HW and L-HW. The nitrogen adsorption–desorption isotherms that were observed in the samples corresponded to what has been described for tension wood cell walls by Chang et al. (2009), where an isotherm of intermediate between type II and type IV confirmed the presence of mesopores that had a broad size distribution and continued into the macropore field.

It is widely accepted that there is a correlation between the type of hysteresis loop and the pore shape. The formation of hysteresis loops at a certain relative pressure indicates the essential multilayer adsorption process characterizing the mesopore structure (He et al. 2004). Pore shape affects the mechanisms of condensation and evaporation. Four types of hysteresis loops have been recognized according to

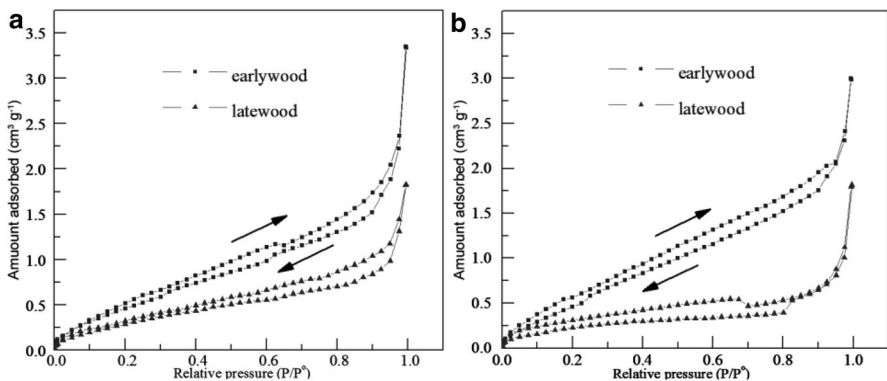


**Fig. 4** Nitrogen adsorption–desorption isotherms in **a** sapwood and **b** heartwood of *Cunninghamia lanceolata*



IUPAC classification (Fig. 1b). Type H1 has been associated with pore materials made from agglomerates or compacts of spheres that are approximately uniform and have a narrow pore size distribution. Type H2 can be found in many pore adsorbents and is believed to occur in systems, where the distribution of pore sizes and pore shapes are broad. Type H3 does not exhibit any limiting adsorption at a high relative pressure, but occurs with aggregates of plate-like particles that give rise to slit-shaped pores. Type H4 is almost horizontal and parallel over a wide range of relative pressure; it is associated with narrow slit-like pores. The hysteresis loop of E-SW in this study (as well as the L-SW, E-HW, and L-HW) was almost vertical and virtually parallel above a relative pressure of 0.9 and failed to reach adsorption saturation, indicating a type H3 with slit-shaped pores (Fig. 4a and b). Such a phenomenon was consistent with the foregoing finding by Chang et al. (2009) that tension wood cell walls of *Sextonia rubra* displayed a type H3 hysteresis loop. Therefore, the micropores and mesopores were slit-shaped pores and existed in both the sapwood and the heartwood.

### Surface area and pore size distribution

The pore volumes and surface areas were slightly different between the sapwood and the heartwood. Detailed pore structure information of the samples is listed in Table 2.  $V_{\text{total}}$  of the earlywood and latewood in the sapwood was greater than that of the heartwood.  $V_{\text{total}}$  of the E-SW and L-SW were 0.0046 and 0.0030  $\text{cm}^3 \text{g}^{-1}$ . The values of  $V_{\text{total}}$  were reduced to 0.0039  $\text{cm}^3 \text{g}^{-1}$  for the E-HW and 0.0024  $\text{cm}^3 \text{g}^{-1}$  for the L-HW, indicating a decrease of 15 and 20 %, respectively. A similar phenomenon was obtained for the  $S_{\text{BET}}$ .  $S_{\text{BET}}$  of the E-SW and L-SW was 2.088 and 1.255  $\text{m}^2 \text{g}^{-1}$ , but the  $S_{\text{BET}}$  of the E-HW and the L-HW was 1.058 and 0.787  $\text{m}^2$

**Table 2** Pore structure parameters of *Cunninghamia lanceolata*

	E-SW	L-SW	E-HW	L-HW	F probability
$S_{\text{BET}}^{\text{a}}$ ( $\text{m}^2 \text{g}^{-1}$ )	2.088 <sup>c</sup> (0.394 <sup>f</sup> )	1.255 <sup>B</sup> (0.337)	1.058 <sup>B</sup> (0.069)	0.787 <sup>B</sup> (0.132)	<0.0019
$S_{\text{micro}}^{\text{b}}$ ( $\text{m}^2 \text{g}^{-1}$ )	0.077 <sup>A</sup> (0.134)	0.068 <sup>A</sup> (0.115)	0.505 <sup>B</sup> (0.019)	0.438 <sup>B</sup> (0.176)	<0.0039
$S_{\text{micro}}/S_{\text{BET}}$	4 %	5 %	48 %	56 %	
$S_{\text{ext}}^{\text{c}}$ ( $\text{m}^2 \text{g}^{-1}$ )	2.011 <sup>A</sup> (0.288)	1.189 <sup>B</sup> (0.337)	0.552 <sup>C</sup> (0.052)	0.349 <sup>C</sup> (0.161)	<0.0001
$V_{\text{total}}^{\text{d}}$ ( $\text{cm}^3 \text{g}^{-1}$ )	4.610*10 <sup>-3</sup> <sup>A</sup> (0.602*10 <sup>-3</sup> )	3.004*10 <sup>-3</sup> <sup>AB</sup> (0.513*10 <sup>-3</sup> )	3.989*10 <sup>-3</sup> <sup>BC</sup> (0.385*10 <sup>-3</sup> )	2.444*10 <sup>-3</sup> <sup>C</sup> (0.599*10 <sup>-3</sup> )	<0.0044

Each datum was calculated from three duplicated samples

E-SW earlywood in sapwood, L-SW latewood in sapwood, E-HW earlywood in heartwood, L-HW latewood in heartwood

<sup>a</sup> BET-specific surface area,  $S_{\text{BET}} = S_{\text{micro}} + S_{\text{ext}}$ ; <sup>b</sup> surface area of the micropores; <sup>c</sup> surface area of the mesopores; <sup>d</sup> total pore volume; <sup>e</sup> same capital letter in the same column of the table indicates that there is no significant difference among the sampling positions at  $P < 0.05$  (LSD multiple comparison analysis); <sup>f</sup> standard deviations

$\text{g}^{-1}$ , respectively, showing a decrease of 49 and 37 %, respectively. On the other hand, it was noted that the  $S_{\text{micro}}$  of the earlywood and latewood in the sapwood was lesser than that in the heartwood.  $S_{\text{micro}}$  of the E-SW was  $0.077 \text{ m}^2 \text{ g}^{-1}$ , and  $S_{\text{micro}}$  of the L-SW was  $0.068 \text{ m}^2 \text{ g}^{-1}$ . The values increased to  $0.505 \text{ m}^2 \text{ g}^{-1}$  for the E-HW and  $0.438 \text{ m}^2 \text{ g}^{-1}$  for the L-HW, an increase of 85 and 84 %, respectively. The ratio of the micropore surface area to the BET-specific surface area ( $S_{\text{micro}}/S_{\text{BET}}$ ) greatly increased from the sapwood to heartwood and was in the order of E-SW < L-SW < E-HW < L-HW.

In order to carry out more analyses of the micropore and mesopore structures during the transformation from the sapwood to heartwood, the pore size distribution was determined by applying the DFT method, which is suitable for analysing micropores and mesopores. The pore size distribution of the E-SW, L-SW, E-HW and L-HW is plotted in Fig. 5. There were micropores and mesopores in samples whose dimensions ranged from 1 to 30 nm. A large number of the pore diameters were <10 nm, which also confirmed results measured using the nitrogen adsorption by Sawabe et al. (1973) and using thermoporosimetry by Grigsby et al. (2013). From Fig. 5, more peaks existed in the scope of the mesopores, especially the dominant peak that reached  $\sim 2.7 \text{ nm}$ , which was large and broad in the sapwood. In the heartwood, the dominant peak reached  $\sim 1.4 \text{ nm}$ , which was within the scope of the micropores, whereas the peak that reached  $\sim 2.7 \text{ nm}$  became small and narrow. Obviously, the number of micropores and mesopores were different between the sapwood and the heartwood. In the sapwood, it was easy to identify a large amount of mesopores, which contained distributions of broad pore sizes. In the heartwood, the micropores increased as the mesopores decreased. This agreed with the observation of the surface areas (Table 2), which was probably due to the filling

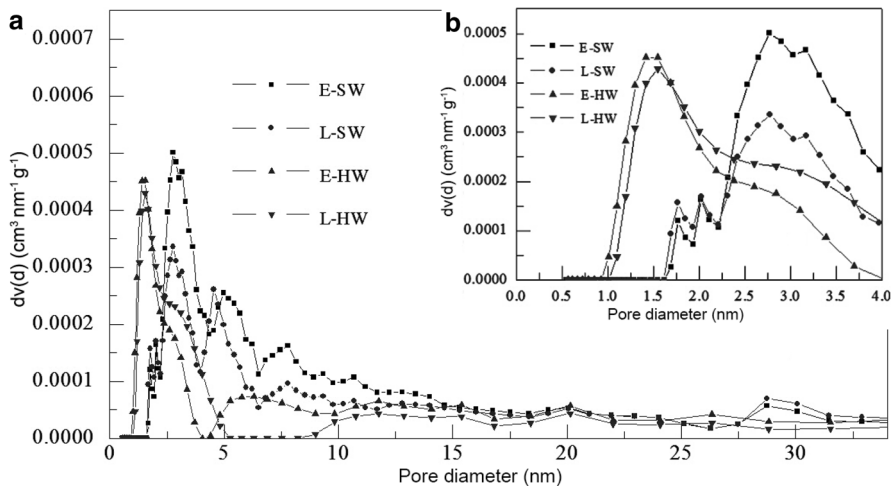


**Fig. 5** Pore size distributions of *Cunninghamia lanceolata* within 30 nm (a). The inset indicates the pore size distributions below 4 nm (b). E-SW earlywood in sapwood, L-SW latewood in sapwood, E-HW earlywood in heartwood, L-HW latewood in heartwood

of pores (the main mesopores) during the heartwood formation (Baron-Epel et al. 1988; Wang et al. 2011).

Furthermore, there were also slight differences among the pore volumes and surface areas when it came to the earlywood and latewood. In the sapwood,  $V_{\text{total}}$  and  $S_{\text{BET}}$  of the E-SW were greater than in the L-SW. However, no significant differences concerning  $S_{\text{micro}}$  were found between the E-SW and the L-SW, which suggested that a large proportion of the  $V_{\text{total}}$  and the  $S_{\text{BET}}$  were attributed to the mesopores in the E-SW. In the heartwood, there were no major distinctions between the E-HW and the L-HW, when it came to the  $V_{\text{total}}$ ,  $S_{\text{BET}}$  and  $S_{\text{micro}}$ , indicating that there were similar micropore and mesopore structures in the E-HW and L-HW.

Pore size distribution curves were similar for the E-SW and L-SW, but the E-SW curve was higher than the L-SW. In particular, the dominant peak, which reached  $\sim 2.7$  nm and corresponded to the mesopores, became greatly increased in the E-SW, suggesting that a greater amount of mesopores existed in the earlywood, when compared to the latewood in the sapwood. However, the pore size distribution curve for the E-HW almost coincided with that for the L-HW, proving that there were no differences in the amounts of micropores and mesopores, when comparing the earlywood with the latewood in the heartwood. These results corresponded to what was described for the surface areas (Table 2). The distinction in the micropores and mesopores when it came to the earlywood and latewood could be linked to the structural features of the wood cell wall and extractives.

### **Mechanism concerning the difference between the sapwood and heartwood in the micropores and mesopores**

As discussed above, more mesopores were found in the sapwood, while the micropores increased with a decrease in mesopores in the heartwood. The significant differences were indicated in the number and size distribution of the micropores and mesopores. Wood cell walls are generally to be regarded as natural fibre biocomposites made up of stiff cellulose, a soft polymer matrix (hemicelluloses and lignin) with extractives and pectins accumulated during the cell growth (Kuo and Arganbright 1980; Sundberg et al. 1996). There are no obvious differences in the main components during the heartwood formation (Song et al. 2014). However, extractives are accumulated in the cell walls during the heartwood formation. It has been suggested that the extractives were derived from the biosynthesis, oxidation and hydrolysis of precursor substances, which appear as lipophilic apolar droplets during the heartwood formation (Hillis 1971; Kampe and Magel 2013; Song et al. 2014). Extractives can form coatings on the cell wall and on the pits and can also penetrate the cell wall itself (Hillis and Melbourne 1968). Furthermore, the amount of pectin, represented by galacturonic acid and rhamnose, increases when heartwood is formed (Bertaud and Holmbom 2004). Thus, the extractives and pectin may be distributed in the mesopores of the cell walls during the heartwood formation, triggering a reduction in the diameter of mesopores in the heartwood cell wall. In addition to the phenomena mentioned above, these are obviously important facts of the improved biological durability of heartwood compared with sapwood.

The differences in the mesopores when it came to the earlywood and latewood in the sapwood could be linked to the structural features of the wood cell wall. Earlywood grows quickly during springtime, when temperatures and photoperiod are favourable for active growth. However, latewood is formed in late summer or autumn, when cambial cell division and expansion decline (Polmion et al. 2001). Latewood has a density 2.3 times greater than earlywood in the sapwood (Dehon et al. 2002). It could be speculated that loose materials in the earlywood that are involved in the early stage probably create more mesopores in the cell wall due to fewer solid substances, leading to there being greater amounts of mesopores in the earlywood, compared with the latewood in the sapwood. However, the small differences that occur in the transition from earlywood to latewood in the heartwood may be closely related to the extractives. During the heartwood formation, phenolic biosynthesis is released and diffused into the neighbouring cell walls and lumens (Streit and Fenge 1994). Extractives are gradually accumulated and probably block the mesopores in the earlywood and latewood of the heartwood. Extractives cannot deposit in micropores of wood cell wall, which results in there being similar amounts of micropores and mesopores in the earlywood and latewood of the heartwood.

## Conclusion

In this study, differences in pore shapes, volumes, surface areas and pore size distributions when it comes to the sapwood and heartwood cell walls were studied using the nitrogen adsorption method. It was indicated that all the samples were an isotherm of intermediate between type II and type IV, confirming the presence of micropores and mesopores in both the sapwood and heartwood, whose dimensions ranged from 1 nm to 30 nm. They were all slit-shaped pores according to the H3 hysteresis loops. However, the number and size distribution of the micropores and mesopores were significantly different when comparing the sapwood to heartwood. There were more mesopores in the sapwood, but the number of the micropores increased in the heartwood, which could be due to the mesopores having been filled. The total volume and BET-specific surface area of the sapwood were greater than those for the heartwood. Furthermore, a greater amount of mesopores existed in the earlywood, when compared to the latewood in the sapwood. However, there was no difference in the amounts of the micropores and mesopores, when it came to the earlywood and latewood in the heartwood.

To a certain degree, research on the micropores and mesopores in the wood cell walls could be significant for tree cultivation and their utilization in the wood processing industry. In order to establish more definitive proof, it is suggested that the following should be studied:

1. An investigation of the individual structures of micropores and mesopores in the various morphological layers of the cell wall (the  $P_1$ ,  $S_1$ ,  $S_2$ ,  $S_3$ ).
2. A detailed investigation of the location of micropores and mesopores in the wood cell walls.

3. An examination of the relationship occurring among the structures of micropores and mesopores and the physical, chemical and mechanical properties of the wood material.
4. An investigation of the structure of micropores and mesopores in modified wood, such as steam treatment (Yin et al. 2011b), hygro-mechanical treatment (Guo et al. 2015), fire retardant, decay resistance. The results would promote an understanding of the effects and mechanism of modified wood, while also providing a scientific basis for the development of environmentally compatible wood products.

**Acknowledgments** This work was supported financially by the Chinese National Natural Science Foundation (No. 31370559 and No. 30972303). We would like to express our gratitude for the assistance on nitrogen adsorption testing given by Mr. Junbo Shang from the College of Materials Science and Technology, Beijing Forestry University, and for assistance with the sample preparation provided by Mrs. Mingkun Xu and Ph.D student Lichao Jiao at the Research Institute of Wood Industry, Chinese Academy of Forestry. We also like to acknowledge the assistance with language editing done by Kevin Austin of BizTech English AB.

## References

- Adam MT, Barbara LG, Jeffrey JM (2002) Heartwood formation and natural durability—a review. *Wood Fiber Sci* 34:587–611
- Aguilera A, Zamora R (2009) Surface roughness in sapwood and heartwood of Blackwood (*Acacia melanoxylon* R.Br.) machined in 90–0 direction. *Euro J Wood Prod* 67:297–301
- Baron-Epel O, Gharyal PK, Schindler M (1988) Pectins as mediator of wall porosity in soybean cells. *Planta* 175:389–395
- Bauch J, Berndt H (1973) Variability of the chemical composition of pit membranes in bordered pits of gymnosperms. *Wood Sci Technol* 7:6–19
- Bertaud F, Holmbom B (2004) Chemical composition of earlywood and latewood in Norway spruce heartwood, sapwood and transition zone wood. *Wood Sci Technol* 38:245–256
- Borrega M, Kärenlampi PP (2011) Cell wall porosity in Norway spruce wood as affected by high-temperature drying. *Wood Fiber Sci* 43:206–214
- Chang S, Clair B, Ruelle J, Beauchene J, Renzo FD, Quignard F, Zhao G, Yamamoto H, Gril J (2009) Mesoporosity as a new parameter for understanding tension stress generation in trees. *J Exp Bot* 60:3023–3030
- Chang S, Hu JB, Clair B, Quignard F (2011) Pore structure characterization of poplar tension wood by nitrogen adsorption-desorption method. *Sci Silvae Sin* 47:134–140
- Dehon L, Macheix JJ, Durand M (2002) Involvement of peroxidases in the formation of the brown coloration of heartwood in *Juglans nigra*. *J Exp Bot* 53:303–311
- Gray RL, Rickey RG, Hergert HL (1983) The influence of sapwood-heartwood conversion of bordered pit tori in western hemlock on bisulfite pulping. *Wood Fiber Sci* 15:251–262
- Grigsby WJ, Kroese H, Dunningham EA (2013) Characterisation of pore size distributions in variously dried *Pinus radiata*: analysis by thermoporosimetry. *Wood Sci Technol* 47:737–747
- Guo J, Song K, Salmén L, Yin Y (2015) Changes of wood cell walls in response to hygro-mechanical steam treatment. *Carbohydr Polym* 115:207–214
- He Y, Li Z, Xi H, Guo J, Xia Q (2004) Research progress of gas-solid adsorption isotherms. *Ion Exch Adsorpt* 20:376–394
- Hillis WE (1968) Chemical aspects of heartwood formation. *Wood Sci Technol* 2:241–259
- Hillis WE (1971) Distribution, properties and formation of some wood extractives. *Wood Sci Technol* 5:272–289

- Huang Z, Tsai CJ, Harding SA, Meilan R, Woeste K (2010) *JnCML-like*, an EF-hand motif-containing gene seasonally upregulated in the transition zone of black walnut (*Juglans nigra* L.). *Plant Mol Biol Rep* 28:222
- Jin Z, Yan X, Yu Y, Zhao G (2014) Sustainable activated carbon fibers from liquefied wood with controllable porosity for high-performance supercapacitors. *J Mater Chem A* 2:11706–11715
- Kampe A, Magel E (2013) New insights into heartwood and heartwood formation. *Cell Asp Wood Form* 20:71–95
- Kojiro K, Miki T, Sugimoto H, Nakajima M, Kanayama K (2010) Micropores and mesopores in the cell wall of dry wood. *J Wood Sci* 56:107–111
- Kuo ML, Arganbright DG (1980) Cellular distribution of extractives in Redwood and Incense Cedar. Part II. microscopic observation of the location of cell wall and cell cavity extractives. *Holzforschung* 34:41–47
- Lu Y, Sun Q, Yang D, She X, Yao X, Zhu G, Liu Y, Zhao H, Li J (2012) Fabrication of mesoporous lignocelluloses aerogels from wood via cyclic liquid nitrogen freezing-thawing in ionic liquid solution. *J Mater Chem* 22:13548–13557
- Nakatani T, Ishimaru Y, Iida I, Furuta Y (2008) Micropore structure of wood: change in micropore structure accompanied by delignification. *J Wood Sci* 54:252–255
- Nakato K (1973) Pore structure of wood (in Japanese). *Mokuzai Gakkaishi* 22:903–907
- Nishida N, Noguchi M, Kuroda K, Ueda M (2014) A design for control of apoptosis in genetically modified *Saccharomyces cerevisiae*. *Biosci Biotechnol Biochem* 78:358–362
- Östlund Å, Köhnke T, Nordstierna L, Nydén M (2010) NMR cryoporometry to study the fiber wall structure and effect of drying. *Cellulose* 17:321–328
- Papadopoulos AN, Hill CAS (2003) The sorption of water vapour by anhydride modified softwood. *Wood Sci Technol* 37:221–231
- Polmion C, Leprovost G, Stokes A (2001) Wood formation in trees. *Plant Physiol* 127:1513–1523
- Qin T, Huang L, Zhou Q (2004) Studies on longitudinal variation of main chemical compositions in Chinese-fir and Poplar × euramaricana1-72/58 trees. *For Res* 17:47–53
- Sawabe O, Kitagawa S (1978) Pore structure in swollen native cellulose: association with structural feature of native cellulose (in Japanese). *Mokuzai Gakkaishi* 24:164–170
- Sawabe O, Mori K, Takeuchi T (1973) Micro-pore structure in cell wall of wood (in Japanese). *Mokuzai Gakkaishi* 19:55–62
- Sing KSW, Everett DH, Haul RAW, Moscou L, Pierotti RA, Rouquerol J, Siemienińska T (1985) Reporting physisorption data for gas-solid systems. *Pure Appl Chem* 57:603–619
- Song K, Liu B, Jiang X, Yin Y (2011) Cellular changes of tracheids and ray parenchyma cells from cambium to heartwood in *Cunninghamia lanceolata*. *J Trop Forest Sci* 23:478–487
- Song K, Yin Y, Salmén L, Xiao F, Jiang X (2014) Changes in the properties of wood cell walls during the transformation from sapwood to heartwood. *J Mater Sci* 49:1734–1742
- Stone JE (1964) The porous structure of wood and fibres. *Pulp Pap Mag Can* 65:3–12
- Stone JE, Scallan AM (1965) A study of cell wall structure by nitrogen adsorption. *Pulp Pap Mag Can* 66:407–414
- Streit W, Fenge D (1994) On the changes of the extractive composition during heartwood formation in Quebrachocolorado (*Schinopsisbalansae* Engl.). *Holzforschung* 48:15–20
- Sundberg A, Sundberg K, Lilland C, Holmbom B (1996) Determination of hemicelluloses and pectins in wood and pulp fibres by acid methanolysis and gas chromatography. *Nord Pulp Pap Res J* 11:216–219
- Thygesen LG, Engelund ET, Hoffmeyer P (2010) Water sorption in wood and modified wood at high values of relative humidity. Part I: results for untreated, acetylated, and furfurylated Norway spruce. *Holzforschung* 64:315–323
- Wang J, Li J, Li S (2011) Components of *Cunninghamia lanceolata* heartwood extracts. *Mater Sci Forum* 685:188–194
- Yin Y, Bian M, Song K, Xiao F, Jiang X (2011a) Influence of microfibril angle on within-tree variation in the mechanical properties of Chinese fir (*Cunninghamia lanceolata*). *IAWA J* 32:431–442
- Yin Y, Berglund L, Salmén L (2011b) Effect of steam treatment on the properties of wood cell walls. *Biomacromolecules* 12:194–202
- Zauer M, Pfriem A, Wagenführ A (2013) Toward improved understanding of the cell-wall density and porosity of wood determined by gas pycnometry. *Wood Sci Technol* 47:1197–1211

- Zauer M, Hempel S, Pfriem A, Mechtcherine V, Wagenführ A (2014a) Investigations of the pore-size distribution of wood in the dry and wet state by means of mercury intrusion porosimetry. *Wood Sci Technol* 48:1229–1240
- Zauer M, Kretschmar J, Großmann L, Pfriem A, Wagenführ A (2014b) Analysis of the pore-size distribution and fiber saturation point of native and thermally modified wood using differential scanning calorimetry. *Wood Sci Technol* 48:177–193
- Zhang Y, Tang Z, He F, Wang M, Zhang B (1997) Characterizing the pore structure of mesoporous activated carbon fiber using nitrogen adsorption isotherms. *Ion Exch Adsorpt* 13:113–119